5

Electromechanical properties of conductive fibres, yarns and fabrics

PU XUE, XIAOMING TAO, MEI-YI LEUNG and HUI ZHANG
The Hong Kong Polytechnic University, Hong Kong

5.1 Introduction

Textiles now play a crucial role in many engineering applications in addition to their initial use as apparel. Intelligent textiles, representing the new generation of fibres, fabrics and articles, are able to sense changes in their environments, such as mechanical, thermal, chemical, electrical, magnetic and optical changes, and then respond to these changes in predetermined ways.[1–3] Currently, many intelligent materials applied in textiles have been developed, such as photonic fibres, shape memory materials, conductive materials, phase change materials, chromic materials, mechanical responsive materials, intelligent coating/membranes, micro and nanomaterials and piezoelectric materials. With the rapid development of the electrical and, particularly, the electronics industry, flexible electrically conducting and semi-conducting materials, such as conductive polymers, conductive fibres, threads, yarns, coatings and ink, are receiving widespread attention. They are playing a more and more important role in realising lightweight, wireless and wearable interactive electronic textiles.

Highly conductive flexible textiles can be prepared by weaving thin wires of various metals such as brass and aluminium. These textiles have been developed for higher degrees of conductivity. Semi-conductive textiles can be produced in various ways, such as by impregnating textile substrates with conductive carbon or metal powders, patterned printing, and so forth. Conducting polymers, such as polyacetylene (PA), polypyrrole (PPy), polythiophene (PTh) and polyaniline (PAn), offer an interesting alternative. Being chemically or electrochemically doped π-conjugated polymers, they have been found to possess metallic properties.[4] Among them, polypyrrole has been widely investigated owing to its good electrical conductivity, good environmental stability in ambient conditions and because it poses few toxicological problems.[5,6] PPy is formed by the oxidation of pyrrole or substituted pyrrole monomers. Electrical conductivity in PPy involves the movement of positively charged carriers or electrons along polymer chains and

the hopping of these carriers between chains. The conductivity of PPy can reach the range 10^2 S cm^{-1}, which is next only to PA and PAn. With inherently versatile molecular structures, PPys are capable of undergoing many interactions.

However, as a conjugated conducting polymer, its brittleness has limited the practical applications of PPy. The processability and mechanical properties of PPy can be improved by incorporating some polymers into PPy.[7,8] However, the incorporation of a sufficient amount of filler generally causes a significant deterioration in the mechanical properties of the conducting polymer, in order to exceed the percolation threshold of conductivity.[9] Another route to overcoming this deficiency is by coating the conducting polymer on flexible textile substrates to obtain a smooth and uniform electrically conductive coating that is relatively stable and can be easily handled.[10,11] Thus, PPy-based composites may overcome the deficiency in the mechanical properties of PPy, without adversely affecting the excellent physical properties of the substrate mterial, such as its mechanical strength and flexibility. The resulting products combine the usefulness of a textile substrate with electrical properties that are similar to metals or semi-conductors.

These products have found wide application in the fields of electromagnetic interference (EMI) shielding, static dissipation, sensing deformation and temperature change, radar-absorbing materials, and so forth.[12–14] They enable the realisation of truly wearable instrumented garments capable of recording surface temperatures and kinetic and dynamic data with no discomfort to the subject and no alteration of signals caused by a mechanical mismatch between the sensor and the body.[15] Currently, some products using interactive electronic textiles have been developed worldwide, such as the Infineon Musical Jacket, Softwitch Electronic Fabrics, Philips Electronic Sportswear Garment, Gorix Electro-Conductive Textile and the Georgia Tech Wearable Motherboard.[16–18] These flexible and ideally conformable products may represent a breakthrough in man–machine interface technology related to virtual reality, teleoperation, telepresence, ergonomics and rehabilitation engineering.[19]

To function as intelligent textiles, the electrical, chemical and mechanical properties of conductive textiles are crucial. Electromechanical behaviour must be thoroughly understood in sensing, actuating and transporting data. In this chapter, we will first briefly introduce conductive textiles, and then focus on the electrical and mechanical properties of PPy-coated conductive fibres/yarn. Based on an understanding of the electrical and mechanical properties of the conductive fibres, the performance of the electrically conductive fabrics will be characterised and evaluated. The relationships between the structural details of the fabric and conductivity will be examined.

5.2 Conductive textiles

Conductive textiles include electrically conductive fibres,[20] fabrics and articles made from them. They can be obtained in various ways.

5.2.1 Metal fibres

Metal fibres can be produced from conductive metals such as ferrous alloys, nickel, stainless steel, titanium, aluminium and copper. Metal fibres are very thin filaments with diameters ranging from 1 to 80 μm. Although highly conductive, metallic fibres are expensive, brittle and heavier than most textile fibres, making it difficult to produce homogeneous blends.

5.2.2 Fibres containing metal, metal oxides and metal salts

Two general methods of coating fibres with conductive metals have been used commercially. One is by chemical plating, the other by dispersing metallic particles at a high concentration in a resin, which is then coated on the surface of the fibre and cured. Semi-conducting metal oxides are often nearly colourless, so their use as conducting elements in fibres has been considered likely to lead to fewer problems with visibility than the use of conducting carbon. The oxide particles can be embedded in surfaces, or incorporated into sheath–core fibres, or react chemically with the material on the surface layer of fibres. Conductive fibres can also be produced by coating fibres with metal salts such as copper sulfide and copper iodide. Metallic coatings produce highly conductive fibres; however adhesion and corrosion resistance can present problems.

5.2.3 Fibres containing conductive carbon

To produce fibres containing conductive carbon, several methods can be used, such as:

- loading the whole fibres with a high concentration of carbon;
- incorporating the carbon into the core of a sheath–core bicomponent fibre;
- incorporating the carbon into one component of a side–side or modified side–side bicomponent fibre;
- suffusing the carbon into the surface of a fibre.

5.2.4 Fibres containing inherently conductive polymers

Based on PAn, PPy and PTh, it is now possible to coat and impregnate conventional fibres with conductive polymers, or to produce fibres from conductive polymers alone or in blends with other polymers.

5.2.5 Conductive yarns and fabrics

Conductive fibres/yarns can be produced in filament or staple lengths and can be spun with traditional non-conductive fibres to create yarns that possess varying

degrees of conductivity. Also, conductive yarns can be created by wrapping a non-conductive yarn with metallic copper, silver or gold foil and be used to produce electrically conductive textiles.

Conductive threads are typically finer and stronger than conductive yarns, with controlled conductivity through the placement of stitches. Conductive threads can be sewn to develop intelligent electronic textiles. Through processes such as electrodeless plating, evaporative deposition, sputtering, coating with a conductive polymer, filling or loading fibres and carbonising, a conductive coating can be applied to the surface of fibres, yarns or fabrics. Electrodeless plating produces a uniform conductive coating, but is expensive. Evaporative deposition can produce a wide range of thicknesses of coating for varying levels of conductivity. Sputtering can achieve a uniform coating with good adhesion. Textiles coated with a conductive polymer, such as PAn and PPy, are more conductive than metal and have good adhesion, but are difficult to process using conventional methods.

Adding metals to traditional printing inks creates conductive inks that can be printed onto various substrates to create electrically active patterns. The printed circuits on flexible textiles result in improvements in durability, reliability and circuit speeds and in a reduction in the size of the circuits. The inks withstand bending and laundering without losing conductivity. Currently, digital printing technologies promote the application of conductive inks on textiles.

5.3 Electromechanical properties of PPy-coated conductive fibres/yarns

In this section, we will focus on the electrical and mechanical properties of PPy-coated conductive fibres/yarns, which will be applied in sensing applications under large and repeated deformation, and also establish a basic understanding for modelling the performance of conductive fabrics.

5.3.1 Experimental details

Materials and the preparation of samples

Considering their potential applications in smart textiles, two material systems were examined in the present study: polycaprolactam (PA6) fibres coated with PPy and polyurethane (PU) fibres (Lycra™) coated with PPy. The commercial multifilaments of PA6 with triangular profile were supplied by Dupont, and multifilament PU yarn was supplied by Sunikorn Knitters Limited (Hong Kong). Pyrrole (99%) and ferric chloride hexahydrate ($FeCl_3.6H_2O$) were purchased from the Sigma-Aldrich Chemical Company. All of the chemicals in the highest available grades were used as received without undergoing any purification. The linear density of the PA6 yarn is 702 denier/68F and that of polyurethane yarn is 40 denier/5F.

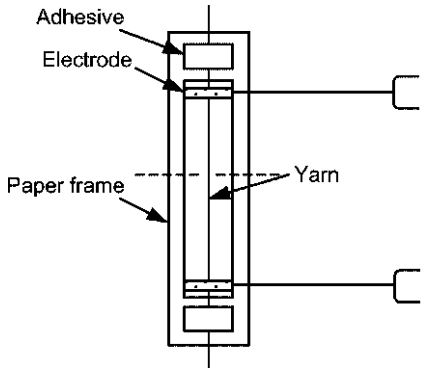

5.1 Schematic drawing of a sample to be tested.

PPy-coated fibres were obtained by the chemical vapour deposition method. The fibres to be coated were fixed parallel each other on a support frame at intervals and soaked in a 50 g L^{-1} $FeCl_3$ solution (used as the oxidising agent) for 10 min. They were then taken out and the residual oxidising solution on the fibre surface was removed by a filter paper. The fibres soaked with oxidising agent were transferred to a glass desiccator in which a beaker containing l0 ml of pyrrole monomer was placed. The desiccator with the fibres and pyrrole was first vacuum-suctioned and then opened to a nitrogen gas atmosphere at room temperature for 24 h. After the vapour deposition process, the PPy-coated fibres were taken out and washed in deionised water for 10 min. They were then put in a desiccator for drying before being measured. Samples of PPy-coated PA6 fibres and PPy-coated PU fibres were both prepared under the same conditions.

Characterisation methods

A scanning electron microscope (SEM) (Lecia Steroscan 440) and a scanning probe microscope (SPM) (API4000/SPA-300HV) were used to observe the surface and cross-section of PPy-coated fibres. The SEM microphotographs were obtained at an accelerating voltage of 5 kV for PPy-coated PU fibres and at a higher accelerating voltage of 20 kV for PPy-coated PA6 fibres. The phase and topographical images were obtained by SPM under ambient conditions.

The electrical resistance of the PPy-coated fibres was measured by the four-probe method with a Keithley 2010 multimeter while the fibres were extended. The load and deformation were obtained and recorded using an Instron mechanical testing system. A single piece of yarn was attached vertically with adhesive (60 mm apart) to a piece of paper with a rectangular hole cut in the centre. Prior to applying a vertical tensile load, the paper was cut horizontally along the dashed line, as shown in Fig. 5.1. The crosshead speed was 5 mm min^{-1} and the gauge length of each specimen was 50 mm. At least five specimens from each sample

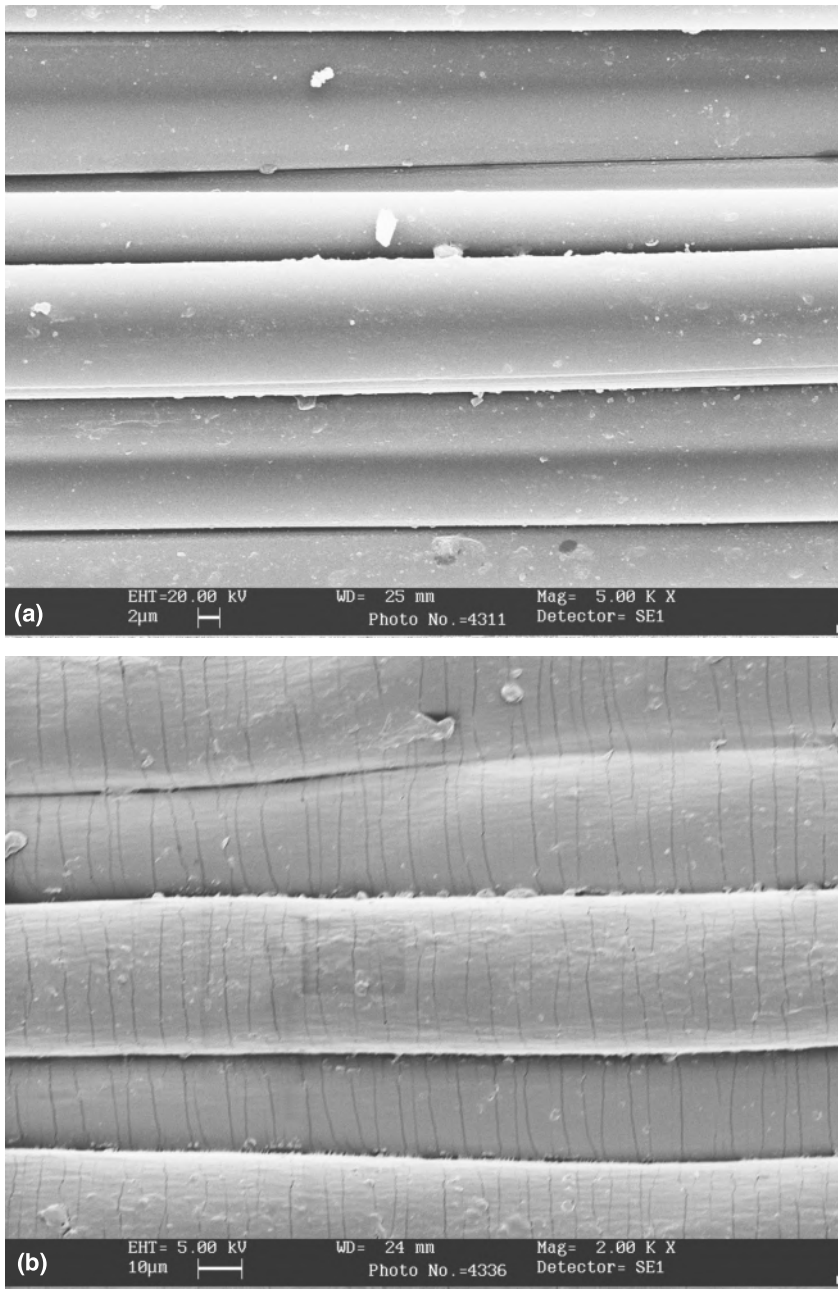

5.2 SEM microphotographs of the (a) PPy-coated PA6 fibres and (b) PPy-coated PU fibres with magnification of 5000 and 2000, respectively.

were tested and the average value was taken. All electromechanical tests were carried out at 20ºC and 65%RH (relative humidity).

5.3.2 Experimental results

Microscale observation

From the SEM images, it is believed that the process described for polymerising pyrrole on the surface of PPy-coated fibres encases each single fibre of the textile assembly. For PA6 fibres, the electrically conductive polymer is in a smooth, coherent layer. For PU fibres, some transverse microcracks occurred on the surface, as shown in Fig. 5.2.

The effect of the substrate material on the conductive coating layer was further confirmed by an SPM observation of the cross-sectional view of the fibres, as shown in Fig. 5.3. A continuous PPy conductive domain of 200–300 nm thickness was observed on the surface of the PA6 fibres, whereas there was a thin and discontinuous PPy coating on the PU fibres. On these images, the substrate fibre is shown in the darker region in Fig. 5.3(a) and the lighter region in Fig. 5.3(b). The polymer used to embed the sample is in the lighter region in Fig. 5.3(a) and the darker region in Fig. 5.3(b). The electrically conductive material is in between.

Electromechanical performance under simple tension

By the electromechanical testing system, the relationship between electrical resistance and deformation was obtained. Figure 5.4 depicts typical electrical resistance versus strain curves of two kinds of samples. For the PPy-coated PA6 fibres, it was found that the electrical resistance increased with the increase in the strain, and the relationship between R/R_0 and strain was almost linear under tensile loading until the specimen fractured. However, for the PPy-coated PU fibres, the change in resistance could be divided into two phases. In the initial phase, the resistance increased gradually, followed by a second phase in which the resistance increased non-linearly and rapidly. For the PPy-coated PU fibres, a percolation threshold value existed and it was noticed that the strain threshold was much smaller than the ultimate strain of the PU fibre. As the strain approached the percolation threshold, the current conductive paths became longer and thinner due to transverse microcracks, resulting in the resistance increasing sharply.

As is well known, a sensing material should possess special characteristics, such as linearity, repeatability, sensitivity, and so forth. Among them, linearity between the input and the output signals is one of the most important characteristics. In general, the strain sensitivity of a sensor is represented by the gauge factor, defined as the fraction of the increment in its electrical resistance $\Delta R/R_0$ per unit strain, that is:

$$K \text{ (gauge factor)} = \frac{\Delta R/R_0}{\varepsilon} \qquad [5.1]$$

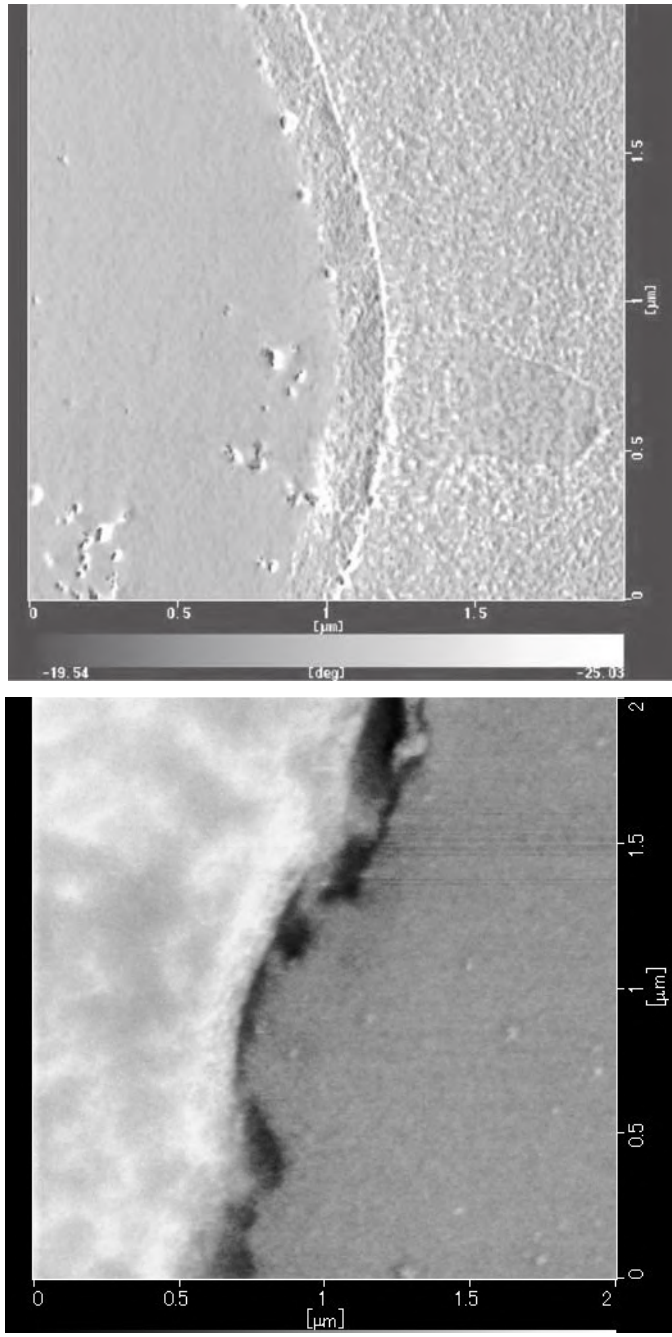

5.3 SPM observation on the cross-sectional view of the fibres, (a) PA6 fibre base; (b) PU fibre base.

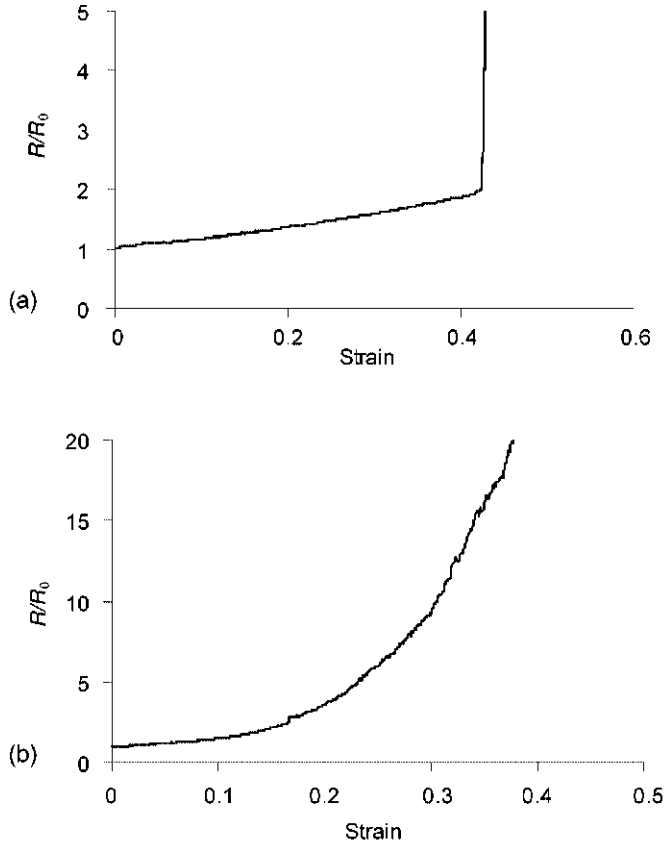

5.4 Typical resistance versus strain curves of (a) PPy-coated PA6 fibres; (b) PPy-coated PU fibres.

where ΔR and R_0 are the change in the resistance and the initial resistance, respectively, and ε is the applied strain. From Fig. 5.5, it was found that the fractional increment in resistance, $\Delta R/R_0$, varies almost linearly with the applied strain, and that the gauge factor of the PPy-coated PA6 fibre is about 2.0 throughout the whole range of strain. Therefore, PPy-coated PA6 fibres possess a good sensing performance. However, as seen from the experimental results shown in Fig. 5.6, PPy-coated PU fibres are not as promising for application as a strain sensor.

The R/R_0 calculated from the change in the dimension of the sample can be calculated from the following equation:

$$R = \rho \frac{L_0}{A_0} \quad \frac{(1+\varepsilon)}{(1-\nu\varepsilon)^2} \qquad [5.2]$$

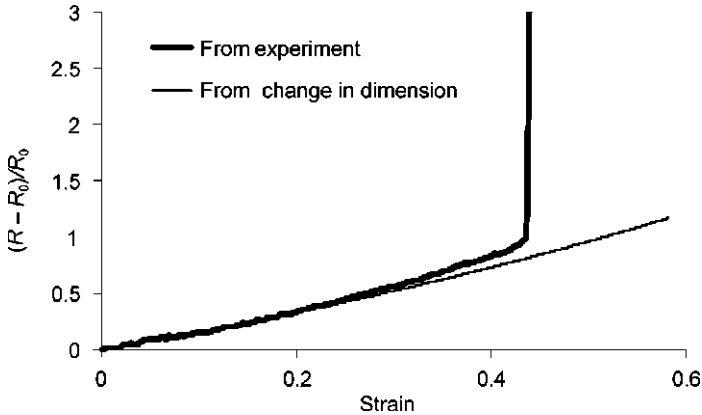

5.5 Typical $\Delta R/R_0$ versus strain curve of PPy-coated PA6 fibres and a comparison of the result calculated from Equation [5.3] and measured from the experiment.

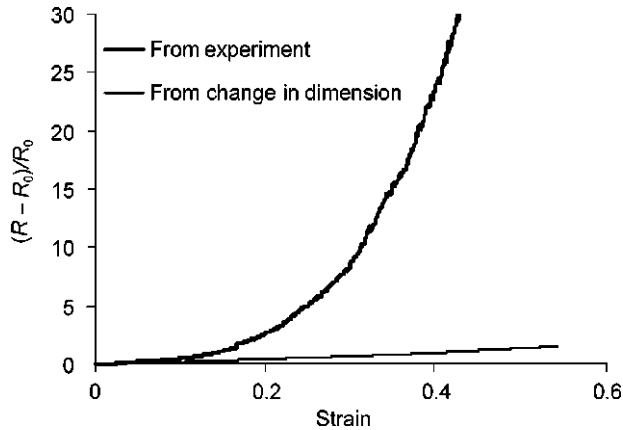

5.6 Comparison of the results of $\Delta R/R_0$ calculated from Equation [5.3] and measured from the experiment for PPy-coated PU fibres.

or

$$R/R_0 = \frac{(1 + \varepsilon)}{(1 - \nu\varepsilon)^2} \qquad [5.3]$$

where R_0 is the initial electrical resistance equal to $\rho_0 L_0/A_0$, and ν is the Poisson's ratio of PPy-coated fibres when elongated along their longitudinal direction.

Several investigators have specifically studied the mechanical properties of PPy. However, the reports from the literature confirm that the mechanical

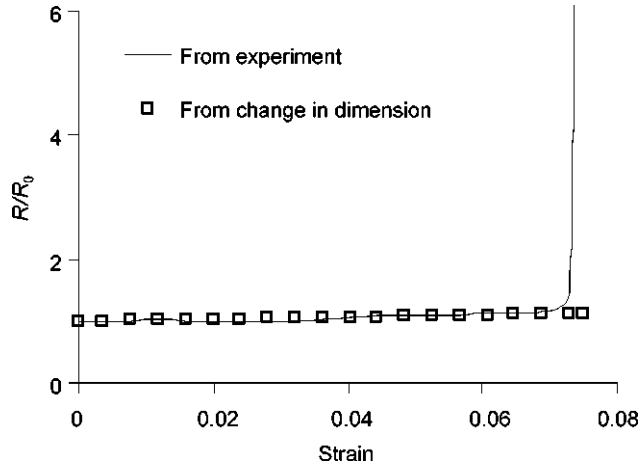

5.7 Comparison of the results of $\Delta R/R_0$ calculated from Equation [5.3] and measured from the experiment for a copper wire.

properties of PPy vary widely from strong, tenacious materials to extremely brittle ones.[4] The composition of the polymer, conditions of polymerisation and the substrate material all have a significant effect on the properties of the polymer. However, owing in part to the intractable nature of PPy film, which makes the characterisation difficult, the relationship is not straightforward. The most commonly reported values are Young's modulus, the tensile strength and the percentage of elongation at break. By taking Poisson's ratio as 0.25 and 0.4 for the PPy-coated PA6 fibre and the PPy-coated PU fibre, respectively, the predictions from Equation [5.3] and measured values of R/R_0 are compared in Figs 5.5 and 5.6. For the PPy-coated PA6 fibres, it was found that the variation in resistance from the change in dimension is slightly smaller than the measured values, but the two curves are quite close to each other when the strain is less than 30%. Therefore, the change in dimension caused by tension is the main cause of the variation in resistance, especially when the applied strain is not large. This behaviour is similar to that of some intrinsically electrically conductive fibres, such as carbon fibres[21] and copper wire, shown in Fig. 5.7. However, the mechanical performance of the PPy-coated fibres is much better than that of these intrinsically electrically conductive fibres. The PPy-coated PA6 fibres provide an excellent sensing performance until the strain of 43%, while intrinsically electrically conductive fibres can only be applied to some situations with small deformation.

In a notable difference from the PPy-coated PA6 fibres, for the PPy-coated PU fibres, the magnitude of $\Delta R/R_0$ caused by the change in dimension only contributes a small percentage of the total variation in resistance and this contribution is further reduced as the applied strain increases. For the PPy-coated PU fibres, the variation in $\Delta R/R_0$ is dominated by the change in its conductivity during tensile deformation.

Performance of conductive fibres under cyclic tension

The sensing function of PPy-coated textiles should be addressed in various environments, such as under cyclic and repeat loads, varying strain rates and temperatures, and so forth. Under cyclic and repeat loading, the electrical resistance may produce a shift, depending on the magnitude of the strain, the number of cycles and the mechanical properties of the carrier employed in a sensor. Figure 5.8 shows typical plots of normalised electrical resistance versus time and applied load versus time for the PPy-coated PA6 fibres, obtained simultaneously during cyclic tension at a maximum strain of 20%, which is equal to 43% of the ultimate strain of the material. From these figures, the applied load was found to have varied consistently as the cyclic number increased. In the first cycle, the electrical resistance increased with loading and decreased with unloading. However, at the end of the first cycle, the electrical resistance could not return to its initial value, R_0. This shift in resistance is attributed to the residual plastic deformation. The shift in electrical resistance is equal to:

$$R_{\text{shift}} = \rho \frac{L_p}{A} \qquad [5.4]$$

where L_p is the length of the conductive fibre when the load is unloaded to zero. For the PPy-coated PA6 fibre, L_p was about 55.9 mm. This resistance remained unchanged until the fibre was again extended. Then, reloading caused the electrical resistance to increase, and subsequent unloading behaved in a manner similar to the first unloading. As cyclic loading progressed, both the applied load and the electrical resistance varied repeatly.

Figure 5.9 shows the variations in electrical resistance and applied load as a function of time during the cyclic tension under various unloading strains. At a strain level lower than 30%, the electrical resistance changed periodically along with the applied load, although there was a different residual resistance after the first unloading. The residual electrical resistance was dependent on the magnitude of the unloading strain and nearly did not change with an increase in the number of cycles. However, if the strain reached 35%, equal to 83% of the ultimate strain, the change in resistance became distorted and no longer varied correspondingly to the load.

For the PPy-coated PU fibres, the repeated tension was performed under a 15% strain level. From the experimental observation described earlier on page 87, it is known that many transverse cracks occur on the surface of the conductive fibres under tension. When applying a cyclic load, electrical resistance increased in loading when the cracks opened, and the resistance returned to its original value after unloading when the cracks closed. In the next cycle, the cracks reopened and reclosed at loading and unloading, causing the electrical resistance to vary abruptly, not gradually, as shown in Fig. 5.10.

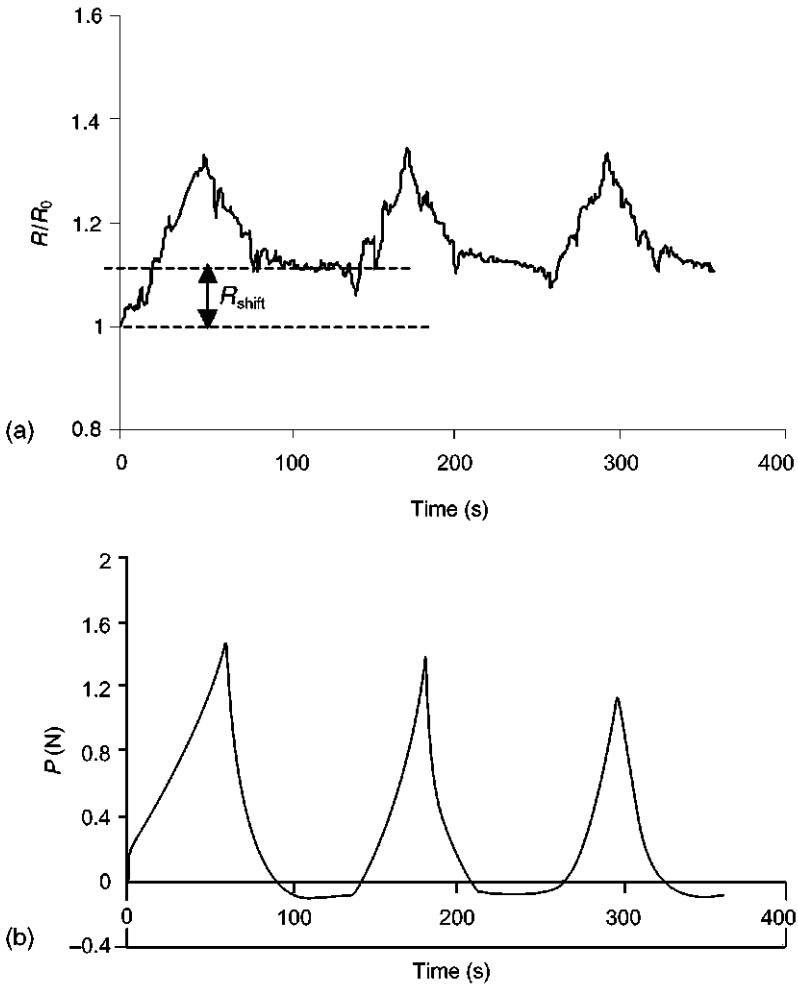

5.8 Variation in (a) electric resistance and (b) applied load during cyclic tension, unloading at strain of 20% (PPy coated PA6 fibres).

Performance of conductive fibres at varying strain rates

Within the capacity of the testing facility, the strain rates examined were 0.17×10^{-3}, 0.17×10^{-2}, 0.17×10^{-1} and 0.17×10^{0} (s^{-1}). A typical group of the load versus strain curves and electrical resistance versus strain curves of the PPy-coated PA6 fibres at different strain rates are given in Fig. 5.11. It is seen that with the increase in the strain rate, the Young's modulus and the strength of the material are enhanced, but the ultimate strain is reduced. Under different strain rates, the change in resistance can be divided into two stages. In the first stage, the relationship between the measured resistance and the applied strain can be

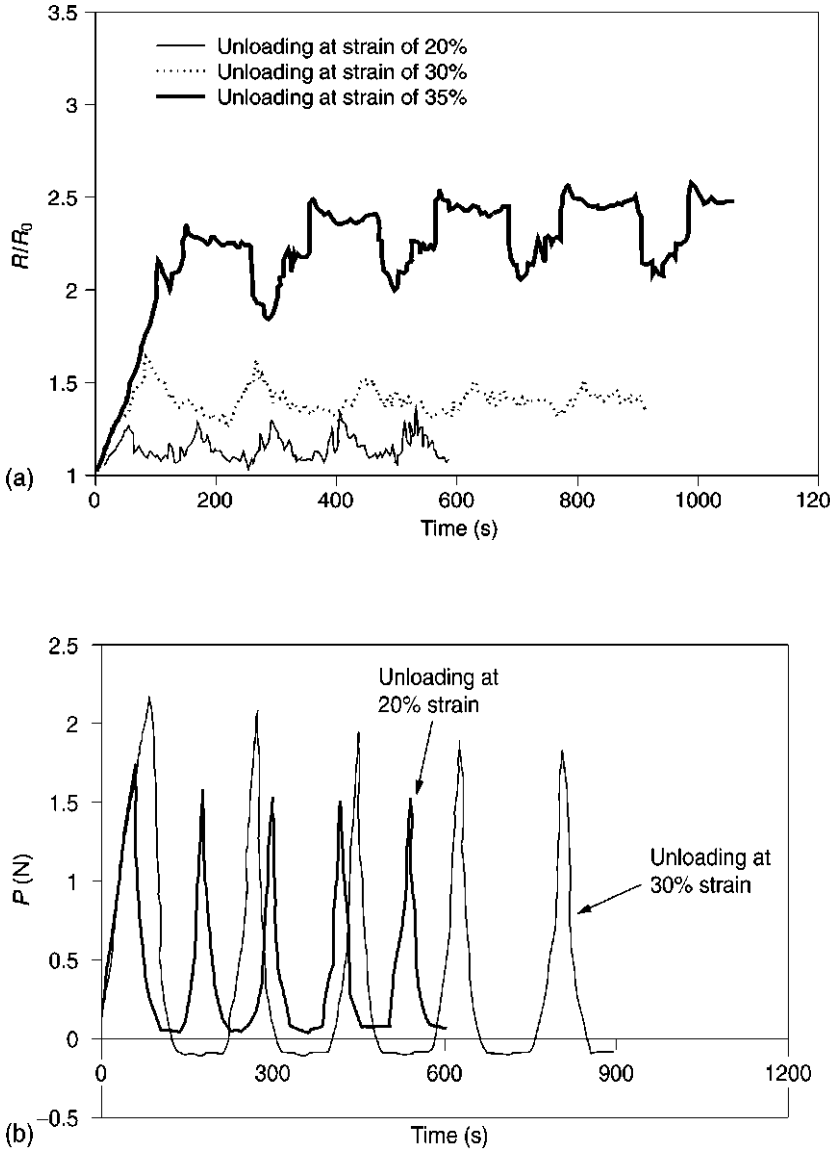

5.9 Variation in (a) electric resistance and (b) applied load during cyclic tension, unloading at different strain levels (PPy-coated PA6 fibres).

reasonably represented by a straight line before a strain threshold, while the threshold appears earlier at higher strain rates. The change in the slope of the straight lines reflects the effect of the strain rate on the performance of conductive fibres. It can be seen that with the increase in the strain rate, the slope of the straight lines increases, while the strain threshold decreases, as shown in Table 5.1.

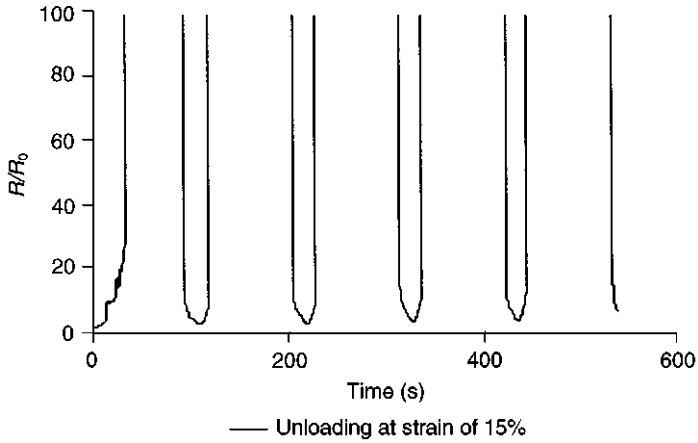

5.10 Variation in electric resistance of PPy coated PU fibres during cyclic tension, unloading at a strain level of 15%.

Table 5.1 Slope and threshold under different strain rates

	Strain rate (s^{-1})			
	0.00017	0.0017	0.017	0.17
Slope of the lines	4.03	4.39	5.43	7.98
Strain threshold	0.52	0.47	0.41	0.22

After a linear range, the electrical resistance increases non-linearly until the fibres rupture. This non-linearity is a result of the accumulated microcracks that occurred on the coating layer. The higher the strain rate, the easier it is for accumulated damage to reach a level sufficient to block electrical conductivity of the material.

5.4 Performance of electrically conductive fabrics

The electromechanical properties of a conductive fabric not only depend on the materials used, but on the structure of the fabric. In this section, the performance of two fabric structures, i.e. PPy-coated plain weave fabric and stainless steel knitted fabric, under uniaxial tension will be reported.

5.4.1 PPy-coated woven fabric under unidirectional tension

A plain weave fabric coated with conducting polymer can be generally represented by an electrical network, as illustrated in Fig. 5.12.[22] The resultant total resistance of the plain weave fabric can be simply expressed as:

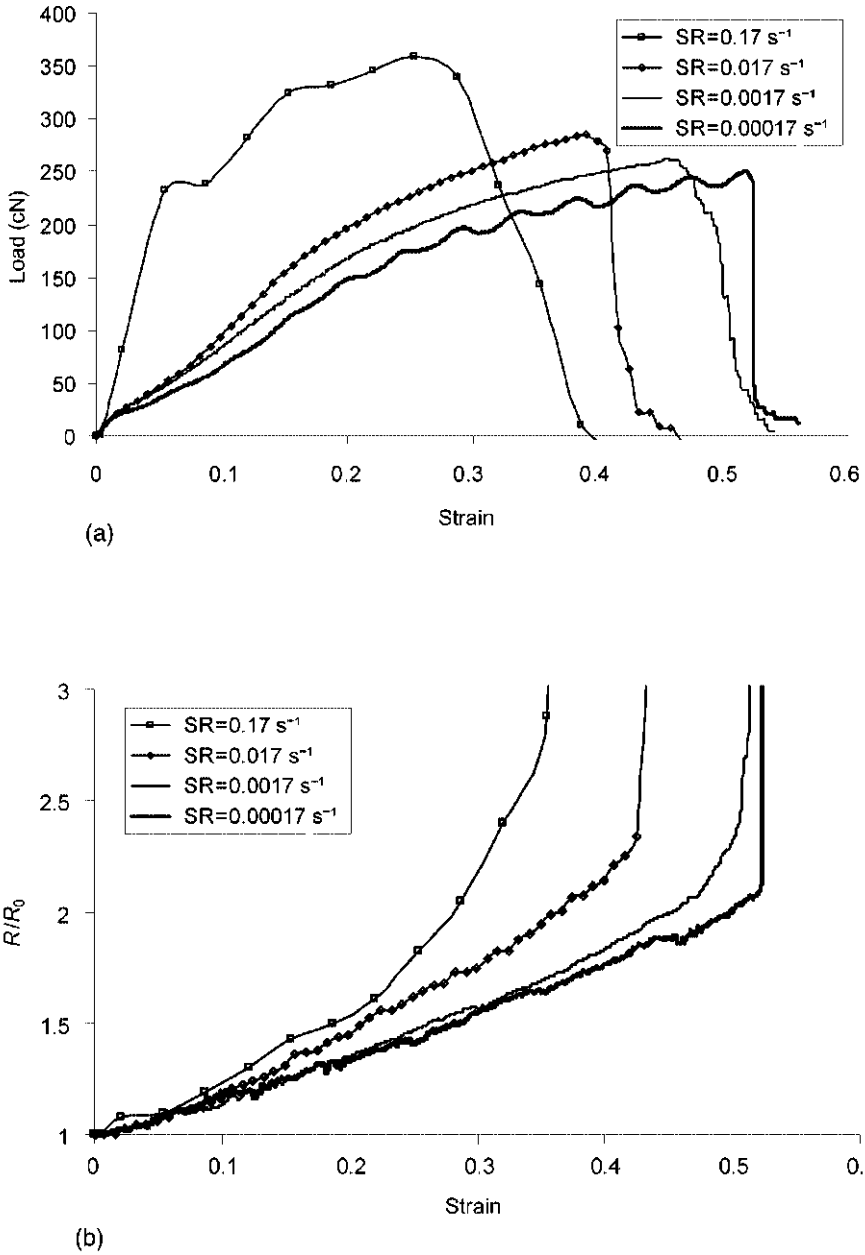

5.11 (a) Load versus strain curves and (b) electrical resistance versus strain curves of PPy-coated PA6 fibres under different strain rates. SR is the strain rate (s^{-1}).

$$\text{Warp direction:} \quad R_v = \frac{\lambda(1 + C_v)(N_p - 1)}{N_e} \qquad [5.5]$$

$$\text{Weft direction:} \quad R_h = \frac{\lambda(1 + C_h)(N_e - 1)}{N_p} \qquad [5.6]$$

where R_v, R_h are the equivalent resultant resistance of the structure measured in the warp and weft directions, respectively; N_p is the number of picks per length and N_e is the number of ends per width; λ is the resistance of yarn per unit length; C_v and C_h are the crimps of the weave in the warp and weft directions, respectively.

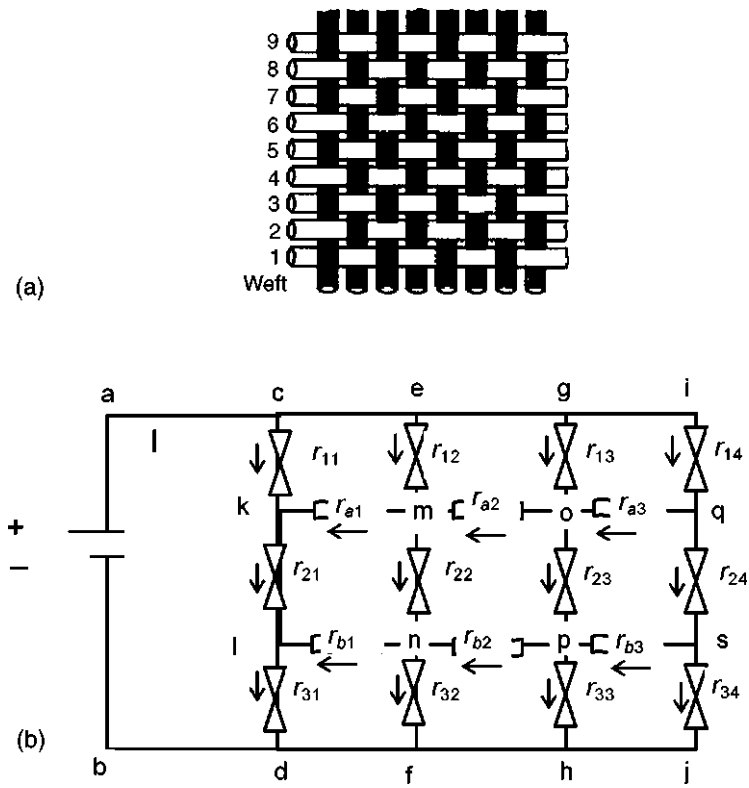

5.12 (a) Plain weave fabric structure. (b) Electrical network representing a segment of the conductive woven fabric.

During the unidirectional tensile deformation (for example in the warp direction), the change in the resistance of the fabric can be expressed as:

$$dR_v = \frac{(N_p - 1)(1 + C_v)}{N_e} d\lambda + \frac{(N_p - 1)\lambda}{N_e} dC_v + \frac{\lambda(1 + C_v)}{N_e} dN_p - \frac{\lambda(N_p - 1)(1 + C_v)}{N_e^2} dN_e \quad [5.7]$$

It can be seen that the change in resistance under large deformation comes from contributions of the yarn and from the geometrical change in the structure of the fabric during tensile deformation, such as change in the crimp of the weave and changes in the densities of the pick and end. Suppose:

$$\lambda = k\varepsilon + \lambda_0 \quad [5.8]$$

then

$$d\lambda = kd\varepsilon \qquad \varepsilon > C_v \quad [5.9]$$

where k is determined from the tensile test of the filaments. Based on the definitions, we have:

$$dC_v = \begin{cases} \dfrac{-(1 + C_v)}{(1 + \varepsilon)^2} d\varepsilon & 0 \le \varepsilon \le C_v \\ 0 & \varepsilon > C_v \end{cases} \quad [5.10]$$

$$dN_p = \frac{-N_{po}}{(1 + \varepsilon)^2} d\varepsilon \quad [5.11]$$

$$dN_e = 0 \quad [5.12]$$

where C_v is the weave crimp of the yarn in the fabric and N_{po} is the original number of picks per fabric length. Substituting Equations [5.8]–[5.12] into Equation [5.7], the gauge factor of the electrical conducting fabric in the warp direction can be determined as:

$$\frac{dR_v}{d\varepsilon} = \begin{cases} -\dfrac{l(1 + C_v)}{(1 + \varepsilon)^2} \left[\dfrac{(N_p - 1)}{N_e} + \dfrac{N_p}{N_e} \right] & 0 \le \varepsilon \le C_v \\ \dfrac{(1 + C_v)(N_p - 1)k}{N_e} - \dfrac{\lambda(1 + C_v)}{(1 + \varepsilon)^2} \dfrac{N_p}{N_e} & \varepsilon > C_v \end{cases} \quad [5.13]$$

The parameters used in Equation [5.7] can be determined experimentally. For PU yarn and a hand-woven fabric, the parameters used in Equation [5.7] are given in Table 5.2.

From Equation [5.13], it is known that the gauge factor of the conductive woven fabric is inversely proportional to $(1 + \varepsilon)^2$. At a small strain level of the fabric

Table 5.2 Parameters used in Equation [5.7]

k	N_{eo} (ends/inch)	N_{po} (picks/inch)	λ_o (kΩ)
0.43 to 0.47	17	17	8.79

N_{eo} is the original number of ends per fabric width.

(before the filaments were extended), $0 \leq \varepsilon \leq C_v$, the gauge factor is mainly governed by the change in the crimp of the weave as well as by the change in the density of the fabric. The negative sign of the gauge factor indicates that the gauge factor increases with the strain in the decrimping process. Under a large deformation (when the strain is greater than the crimp of the weave), $\varepsilon > C_v$, the gauge factor will be affected by both the variation in the density of the pick and the change in the resistance of the filaments.

5.4.2 Electromechanical properties of stainless steel knitted fabric made from multifilament yarn

An electrically conductive knitted fabric can be depicted as a circuit network, as shown in Fig. 5.13, based on following assumptions:[23]

- filaments are intrinsically conductive and conductivity is a constant that is independent of tensile deformation;
- conductivity at the overlapped points of yarns is related only to the normal force applied;
- the friction of the yarn is negligible;
- two-dimensional hexagon geometry can be used.

The intrinsic resistance of the metallic yarn and the contact resistance both contribute to the electrical properties of the fabric. The intrinsic resistance of the

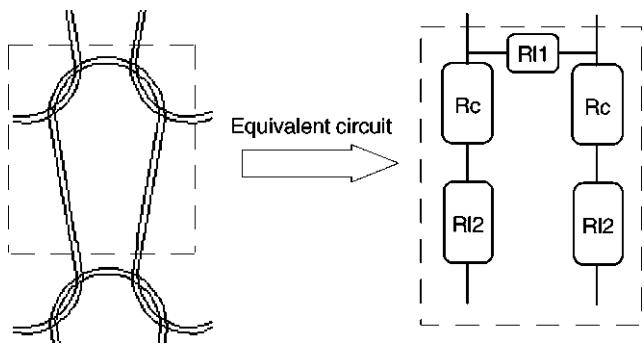

5.13 Circuit network representing a unit loop of the conductive knitted fabric.

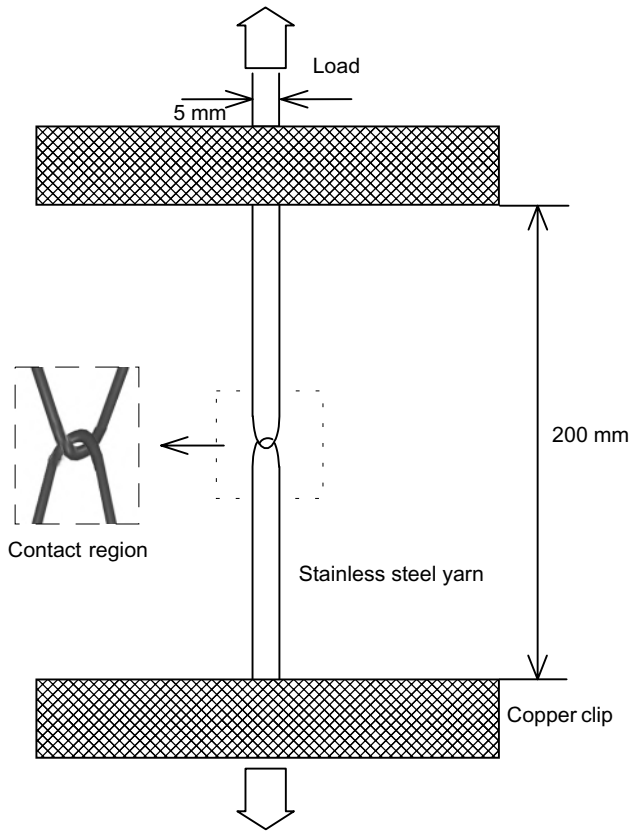

5.14 Experimental setup to measure the contact resistance and contact force at the overlapped point.

metallic yarn can be calculated by Ohm's law and the contact resistance can be determined experimentally. The experimental setup for measuring the contact resistance and contact force is shown in Fig. 5.14. The equivalent resistance of the fabric can then be obtained based on the circuit network.

Based on the experimental results, as shown in Fig. 5.15, it was found that the contacting resistance at the overlapped points decreased with loading. The relationship between the normal force on the two hooked yarns and the contacting resistance can be obtained by the following function:

$$R_c = f(N) \qquad [5.14]$$

where function f was determined experimentally and N is the normal force at the overlapped points.

The equivalent resistance of the fabric can then be obtained based on the circuit

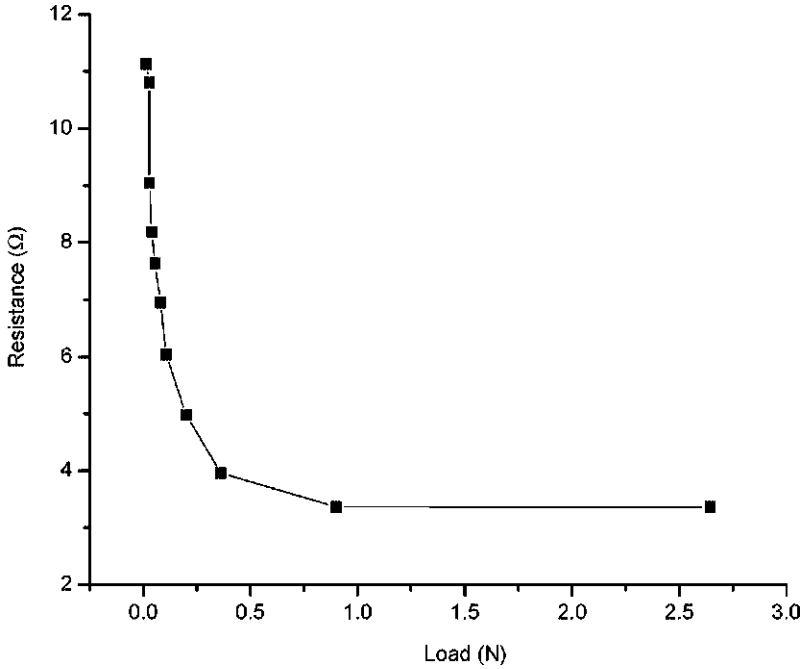

5.15 Contacting resistance versus applied load.

network. The resistances plotted against the load from the experiment and prediction are given in Fig. 5.16. It was found that the contacting resistance at the overlapped points in the knitted fabric governed the change in resistance. The contacting resistance plays a very important role in the sensitivity of the knitted fabric sensor.

5.5 Applications

Electrically conductive textiles make it possible to produce interactive electronic textiles. They can be used for communication, entertainment, health care, safety, homeland security, computation, thermal purposes, protective clothing, wearable electronics and fashion. The details of the applications are listed as follows:[24, 25]

- location/position: infant/toddler/active child monitoring, geriatric monitoring, integrated GPS (global positioning system) monitoring, livestock monitoring, asset tracking, etc.
- infotainment: integrated compact disc players, MP3 players, cell phones and pagers, electronic game panels, digital cameras, and video devices, etc.
- environmental response: colour change, density change, heating change, etc.
- biophysical monitoring (strategic/qualitative assessment only): cardiovascular monitoring, monitoring the vital signs of infants, monitoring clinical trials, etc.

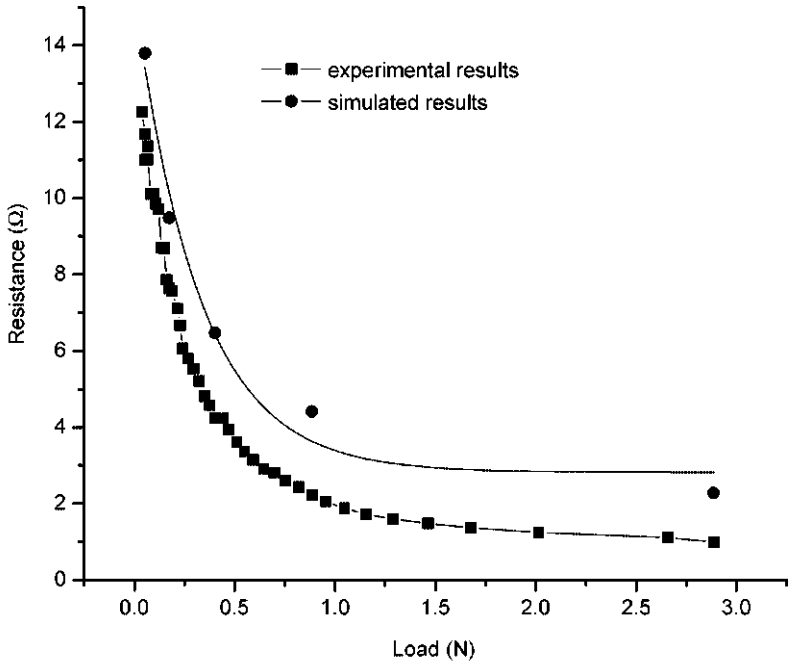

5.16 Comparison of the experimental result and the prediction.

- consumer: health and fitness (professional and amateur; indoor and outdoor activities), home healthcare, fashion, gaming, residential interior design, etc.
- government: military (soldiers, support personnel in the battlefield), space programmes, public safety (fire fighting, law enforcement), etc.
- medical: hospitals, medical centres, assisted-living units, etc.
- commercial: commercial interior design, retail sites, etc.
- industrial: protective textiles, automotive, exposure-indicating textiles, etc.

5.6 Conclusions

This study mainly investigates the electromechanical behaviour of electrically conductive fibres/yarns and fabrics. The following conclusions can be drawn:

- For PPy-coated PA6 fibres, the relationship between the fractional increment in resistance, $\Delta R/R_0$, and the applied strain is reasonably linear within a large strain range, which is of practical importance in sensing applications.
- The variation in resistance for the PPy-coated PA6 fibres results from the change in the dimension of the fibres. By contrast, the variation in resistance with the applied strain for PPy-coated PU fibres is mainly due to damage on the coating layer.
- The strain sensitivity of the conductive woven fabric is inversely proportional

to $(1 + \varepsilon)^2$. Under a low strain level, the gauge factor is mainly governed by the crimp of the weave and density of the fabric. Under a large deformation, it will be affected by both the density of the pick and the change in the resistance of the yarns.

- The contacting resistance in knitted fabric was much larger than the filament resistance itself. The sensitivity of the knitted fabric sensor mainly depends on the contacting resistance and the structure of the fabric.

5.7 Acknowledgement

The financial support extended by the Hong Kong Innovation and Technology Fund is greatly appreciated.

5.8 References

1. Tao X M, *Smart Fibres, Fabrics and Clothing*, Woodhead Publishing, England, 2001.
2. Culshaw B, *Smart Structures and Materials*, Artech House, USA, 1996.
3. Seinivasan A V and Mcfarland D M, *Smart Structures*, Cambridge University Press, UK, 2001.
4. Wallance G G, Spinks M G, Kane-Maguire L A P and Teasdale P R, *Conductive Electroactive Polymers*, CRC Press, New York, 2003.
5. Thiéblemont J C, Brun A, Marty J, Planche M F and Calo P, 'Thermal analysis of polypyrrole oxidation in air', *Polymer*, 1995, **36**, 1605–1610.
6. Omastova M, Pavlinec J, Pionteck J and Simon F, 'Synthesis, electrical properties and stability of polypyrrole-containing conducting polymer composites', *Polym. Int*., 1997, **43**(2), 109–116.
7. Ruckenstein E and Chen J H, 'Polypyrrole conductive composites prepared by coprecipitation', *Polymer*, 1991, **32**(7), 1230–1235.
8. Truong V-T, Riddell S Z and Muscat R F, 'Polypyrrole based microwave absorbers', *J. Mater. Sci.*, 1998, **33**(20), 4971–4976.
9. Chen Y P, Qian R Y, Li G and Li Y, 'Morphological and mechanical behaviour of an in situ polymerised polypyrrole/Nylon 66 composite film', *Polym. Commun*., 1991, **32**(6), 189–192.
10. Gregory R V, Kimbrell W C and Huhn H H, 'Electrically conductive non-metallic textile coatings', *J. Coated Fabrics*, 1991, **20**(1), 167–175.
11. Heisey C L, Wightman J P, Pittman E H and Kuhn H H, 'Surface and adhesion properties of polypyrrole-coated textiles', *Textile Res. J*., 1993, **63**(5), 247–256.
12. Kim M S, Kim H K, Byun S W, Jeong S H, Hong Y K, Joo J S, Song K T, Kim J K, Lee C J and Lee J Y, 'PET fabric/polypyrrole composite with high electrical conductivity for EMI shielding', *Synth. Met*., 2002, **126**(2–3), 233–239.
13. Xue P, Tao X M, Yu T X, Kwok W Y and Leung M Y, 'Electromechanical behaviour of fibres coated with electrically conductive polymer', *Textile Res. J*., 2004, **74**(10), 929–936.
14. Hans H and Child A D, 'Electrically conducting textiles', in *Handbook of Conducting Polymers*, 2nd edn, rev. and expanded, 1998, 993–1013.
15. De Rossi D, Della Santa A and Mazzoldi A, 'Dressware: wearable piezo- and thermo-resistive fabrics for ergonomics and rehabilitation', *Proceedings 19th International Conference-IEEE/EMBS*, Chicago, USA, 1997, 1880–1883.

16. http://www.tut.fi/units/ms/teva/projects/intelligenttextiles/
17. *New Nomads* – An Exploration of Wearable Electronics by Philips, 010 Publisher, Rotterdam, 2000.
18. http://www.softswitch.co.uk/
19. De Rossi D, Della Santa A and Mazzoldi A, 'Dressware: wearable hardware', *Mater. Sci. Eng. C*, 1999, **7**, 31–35.
20. Marchini F, 'Advanced applications of metallized fibres for electrostatic discharge and radiation shielding', *J. Coated Fabrics*, 1991, **20**, 153–166.
21. Cho J W and Choi J S, 'Relationship between electrical resistance and strain of carbon fibres upon loading', *J. Appl. Polym. Sci.*, 2000, **77**, 2082–2087.
22. Leung M Y, Tao X M, Yuen, C W and Kwok W Y, 'Strain sensitivity of polypyrrole-coated fabrics under unidirectional tensile deformation', submitted to *Textile Res. J.*, 2004.
23. Zhang H, Tao X M, and Wang S Y, 'Electro-mechanical properties of stainless steel knitted fabric made from multi-filament yarn under uniaxial extension', submitted to *Textile Res. J.*, 2004.
24. http:// www.vdc-corp.com/
25. Meoli D and May-Plumlee T, 'Interactive electronic textile development: a review of technologies', *J. Textile Apparel, Technol. Management*, 2002, **2**(2), 1–12.